

The Density Effect for the Ionization Loss in Various Materials*

R. M. STERNHEIMER

Brookhaven National Laboratory, Upton, New York

(Received July 2, 1952)

The density effect for the ionization loss of charged particles has been calculated for a number of metals, scintillating materials, gases at various pressures, and photographic emulsion, using a dispersion model involving an appropriate number of dispersion oscillators for each substance. The results are presented in the form of graphs which can be used to correct the ionization loss for the density effect. The theoretical curves for silver chloride and anthracene are in reasonable agreement with experiments on the ionization loss of μ -mesons. A general derivation of the equations for the density effect is given.

I. INTRODUCTION

THE reduction in the ionization loss of charged particles due to the polarization of the medium has been first treated quantitatively by Fermi.¹ In Fermi's treatment it was assumed that the dispersive properties of the medium can be described as due to a single type of dispersion oscillator. Halpern and Hall² showed that the reduction in ionization loss depends strongly on the description of the dielectric properties of the medium. Fermi's equations were extended to the general case of an arbitrary number of dispersion oscillators by Halpern and Hall,³ Wick,⁴ and the present author.^{5,6} Halpern and Hall³ have given values of the density correction for a few substances. More recently, the reduction in ionization loss has been the object of several experiments.⁷ These investigations confirm the existence of the density effect and are in approximate agreement with theory. However, some of the experiments use substances for which the effect has not been calculated, in particular the work of Whittemore and Street⁷ on the ionization loss of μ -mesons in a silver chloride crystal and the work of Bowen and Roser⁷ on the response of anthracene crystals to μ -mesons. Therefore, it appeared worth while to calculate the density effect for silver chloride, anthracene, and for other substances which are likely to be used in future experiments. The results of this work are presented in the first part of this paper. In addition to values of the density effect correction, we have calculated the ionization loss of μ -mesons and electrons in some of the materials for which the density effect is evaluated. Equations are given from which the ionization loss can be readily calculated for the materials whose density effect has been obtained. The theoretical values of the density effect for silver chloride and anthracene are found to be

in reasonable agreement with the experiments.⁷ The second part of the paper gives the derivation of the equations for the density effect which has been previously obtained.⁵ The derivation involves fewer approximations than are made in the theory of Halpern and Hall³ and the result obtained is more general, although there are no essential differences between the two results in most practical cases.

II. CALCULATIONS OF THE DENSITY EFFECT

As shown in the following section, the reduction in the ionization loss $\Delta dE/dx$ (dE = energy loss in distance dx) is

$$\frac{dE}{dx} = \frac{2\pi n e^4}{m v^2} \left[\sum_i f_i \ln \left[\frac{(\bar{\nu}_i^2 + l^2)}{\bar{\nu}_i^2} \right] - l^2 (1 - \beta^2) \right], \quad (1)$$

where n is the number of electrons per cc, m is the electron mass, $v = \beta c$ is the velocity of the passing particle, f_i is the oscillator strength of the i th transition, whose frequency is $\bar{\nu}_i$, l is a frequency which is the solution of the following equation:

$$\frac{1}{\beta^2} - 1 = \sum_i \frac{f_i}{\bar{\nu}_i^2 + l^2}. \quad (2)$$

Here $\bar{\nu}_i$ is to be expressed in terms of the plasma frequency of the medium given by

$$\nu_p = (n e^2 / \pi m)^{1/2}. \quad (3)$$

The $\bar{\nu}_i$ must be obtained for each case from the energy levels of the atoms considered. As a first approximation, the frequencies are given by the ionization potentials $h\nu_i$ of the K , L , M , \dots shells and the f_i are equal to the corresponding occupation numbers divided by the atomic number Z . The ionization potentials were obtained from the table given by Sommerfeld.⁸ For the outermost shell, the tables of Bacher and Goudsmit⁹ were also used. With the ν_i thus obtained, the geometrical mean ν_m of the frequencies is calculated; we have

$$\ln \nu_m = \sum_i f_i \ln \nu_i. \quad (4)$$

⁸ A. Sommerfeld, *Atomic Structure and Spectral Lines* (Methuen and Company, London, 1934), third edition, p. 237.

⁹ R. F. Bacher and S. Goudsmit, *Atomic Energy States* (McGraw-Hill Book Company, Inc., New York, 1932).

* Work done under the auspices of the AEC.

¹ E. Fermi, *Phys. Rev.* **57**, 445 (1940).

² O. Halpern and H. Hall, *Phys. Rev.* **57**, 459 (1940).

³ O. Halpern and H. Hall, *Phys. Rev.* **73**, 477 (1948).

⁴ G. C. Wick, *Nuovo cimento* (9), **1**, 302 (1943).

⁵ R. M. Sternheimer, thesis, University of Chicago (1946) (unpublished).

⁶ See also, A. Bohr, *Kgl. Danske Videnskab. Selskab, Mat.-fys. Medd.* **24**, No. 19 (1948).

⁷ F. L. Hereford, *Phys. Rev.* **74**, 574 (1948); W. L. Whittemore and J. C. Street, *Phys. Rev.* **76**, 1786 (1949); F. Bowen and F. X. Roser, *Phys. Rev.* **85**, 992 (1952).

A check on the value of ν_m is provided by the determination of the average ionization potential I which occurs in the Bethe-Bloch stopping power formula,¹⁰

$$\frac{dE}{dx} = \frac{4\pi n e^4}{m v^2} \left[\ln \frac{2 m v^2}{I(1-\beta^2)} - \beta^2 \right]. \quad (5)$$

In their recent measurement of the stopping power of 340-Mev protons, Bakker and Segrè¹¹ have obtained values of I for a number of elements. According to the Bloch theory I should be proportional to Z . Bakker and Segrè confirm this dependence for $Z > 26$, where I is approximately given by

$$I = 9.4Z \text{ ev.} \quad (6)$$

For smaller Z , the values of I are somewhat larger than given by Eq. (6). The mean of the frequencies should equal I/h . It was found for all cases that the values of ν_m obtained from the ionization potentials must be increased by a factor of order 1.3 to give agreement with I/h . Thus for Ag, the ν_i correspond to the following ionization potentials: 1878 ry, 260 ry, 36.3 ry, 4.82 ry, 0.55 ry for the $n=1, 2, 3, 4, 5$ shells, respectively (n

=principal quantum number). The f_i are 2/47, 8/47, 18/47, 18/47, 1/47. The resulting $h\nu_m$ is 25.2 ry, which is a factor 1.25 lower than the experimental value¹¹ of 31.5 ry. To obtain the frequencies to be used in Eq. (1) the ν_i obtained from the ionization potentials were raised by the factor 1.25. This procedure was carried out for each substance. In the following, the experimental mean frequency is denoted by ν_m' and the corrected transition frequencies are denoted by ν_i' , so that

$$\nu_i' = (\nu_m'/\nu_m)\nu_i. \quad (7)$$

The factor ν_m'/ν_m is perhaps an indication that the average of the states to which the electrons are excited lies in the continuum above the ionization limit. The values of $\bar{\nu}_i$ used in Eq. (1) are obtained from

$$\bar{\nu}_i = \nu_i'/\nu_p. \quad (8)$$

The solids for which the density effect is obtained include gold, photographic emulsion, anthracene, silver chloride, in addition to the metals investigated by Bakker and Segrè.¹¹ For the gases, we have calculated cases at high pressure for possible application to experiments with diffusion and expansion cloud chambers. The results for H₂ and A at 0.2 atmos are included on account of their use in counters. The results are shown in Figs. 1 and 2, in which the quantity in brackets of Eq. (1),

$$\delta = \sum_i f_i \ln((\bar{\nu}_i^2 + l^2)/\bar{\nu}_i^2) - l^2(1-\beta^2), \quad (9)$$

is plotted against $\log_{10}(p/\mu c)$, where p is the momentum and μ is the mass of the passing particle. This semilog plot was used because δ is then approximately a straight line at large $p/\mu c$. The data which were used to calculate δ are given in Table I. In this table are listed the ionization potentials $h\nu_i$ (in ry units), the resulting mean excitation potential $h\nu_m$, the experimental value $h\nu_m'$, and the factor ν_m'/ν_m by which the ν_i are multiplied to give the ν_i' . The table also shows the oscillator strengths f_i and the plasma energy $h\nu_p$. The last two rows give the constants A and B [see Eqs. (13a, b)] which are useful in calculating the ionization loss. In cases for which ν_m' was not obtained experimentally, it was obtained by interpolation from Table I of Bakker and Segrè.¹¹

In cases of compounds the frequencies for the component atoms are listed. For anthracene and toluene ν_1, ν_2, ν_3 pertain to C, and ν_4 pertains to H. The values of $h\nu_m'$ listed are the geometric means of the $h\nu_m'$ for the component atoms and are the values to be used in the Bethe-Bloch formula. The factors by which the ν_i are multiplied are given in the tables for graphite and H₂. For H₂O, ν_1, ν_2, ν_3 pertain to O, and ν_4 pertains to H. For O, we have $h\nu_m = 6.14$ ry, $h\nu_m' = 7.26$ ry, $\nu_m'/\nu_m = 1.18$. For AgCl, $\nu_1-\nu_5$ refer to electrons bound in Ag atoms and $\nu_6-\nu_8$ refer to Cl. The factor ν_m'/ν_m for Ag is 1.25 (see table for silver), while for Cl, $h\nu_m = 11.8$ ry, $h\nu_m' = 13.5$ ry, so that $\nu_m'/\nu_m = 1.14$. Thus $h\nu_1'$ for $n=1$ of Ag is $(1878)(1.25) = 2348$ ry, and $h\nu_8'$ for $n=1$ of

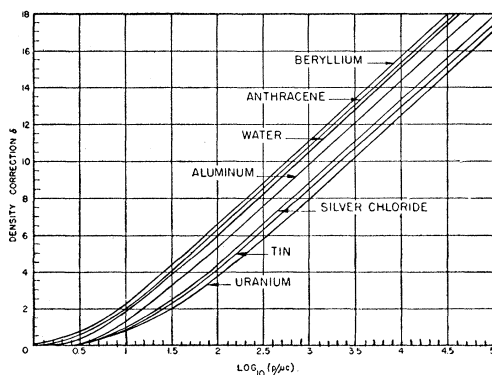


FIG. 1. Density effect correction δ for condensed materials as a function of the momentum/mass of the passing particle.

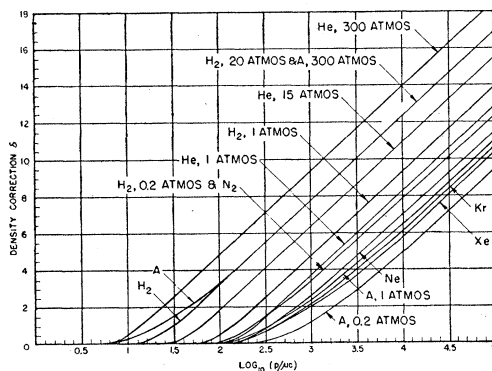


FIG. 2. Density effect correction δ for gases as a function of the momentum/mass of the passing particle.

¹⁰ M. S. Livingston and H. A. Bethe, *Revs. Modern Phys.* **9**, 285 (1937).

¹¹ C. J. Bakker and E. Segrè, *Phys. Rev.* **81**, 489 (1951).

Cl is (208)(1.14) = 237 ry. The $h\nu_i'$ are then divided by $h\nu_p = 3.33$ ry. In calculating δ for photographic emulsion, it was assumed that 47 percent of the oscillator strength is due to Ag, 33 percent to Br, and 20 percent to N. The small amount (1.2 percent) iodine was lumped with the silver, and the dispersive characteristics of the light elements, mostly O, C, and H were taken to be those of N. Only the $h\nu_i$ of Br are listed; the frequencies for Ag and the light elements can be found in the tables for silver and N₂, respectively. For Br, $h\nu_m = 21.1$ ry, $h\nu_m' = 24.2$ ry, so that the factor $\nu_m'/\nu_m = 1.15$. The value listed $h\nu_m' = 21.0$ ry is the geometric mean appropriate for emulsion.¹² For NaI, $\nu_1 - \nu_5$ pertain to I, while $\nu_6 - \nu_8$ pertain to Na. For I, $h\nu_m = 29.7$ ry, $h\nu_m' = 36.6$ ry, so that the values of ν_i were increased by a factor 1.23. For Na, the corresponding energies are $h\nu_m = 6.73$ ry, $h\nu_m' = 9.57$ ry, so that $\nu_m'/\nu_m = 1.42$.

For a gas at a pressure of P atmos, $h\nu_p$ is $P^{1/2}$ times the value of $h\nu_p$ at 1 atmos, listed in Table I. Correspondingly, $\bar{\nu}_i^2$ in Eq. (2) is reduced by a factor $1/P$. Thus, the value of β for which the density effect sets in is raised as P is increased. The appropriate $\beta = \beta_0$ is given by

$$\beta_0 = (1 + \sum_i f_i / \bar{\nu}_i^2)^{-1/2} \quad (9a)$$

Figure 2 shows the increase of the density effect as the pressure is raised. This effect corresponds to the increase of the polarization as the density is increased.

Figures 1 and 2 also show a general decrease of δ with increasing Z . As the atomic number increases, the electrons are more strongly bound and hence are less effective in polarizing the medium. Thus for two substances with the same n , δ is smaller for the one with larger Z . Some of the curves of δ for condensed materials are not shown in Fig. 1 because they closely coincide with curves that are on this figure. The curve for Li lies ~ 0.13 below the Be curve in the region of large $p/\mu c$ where δ is linear. The curve for toluene is ~ 0.2 below the anthracene curve. It may be noted that stilbene, terphenyl, and phenylcyclohexane (C₆H₅C₆H₁₁) have about the same δ as anthracene, while the toluene curve also applies to benzene. The curve for xylene lies ~ 0.1 below the anthracene curve. δ for graphite is 15.6 at $p/\mu c = 10^4$; the curve lies ~ 0.19 above the anthracene line for large $p/\mu c$. δ for polyethylene practically coincides with the curve for graphite.

The values of δ for Fe and Cu lie close to the Al curve. δ for Fe is about the same as for Al for large $p/\mu c (> 10^2)$ and is ~ 0.12 higher at $p/\mu c = 10^{1.5}$. The Cu curve lies close to the Al curve for low momenta and is ~ 0.10 below it for large $p/\mu c (> 10^3)$. δ for silver is ~ 0.2 above the AgCl curve. δ for emulsion is ~ 0.1 above the AgCl curve. δ for Au is ~ 0.07 higher than δ for Sn, while δ for W is ~ 0.18 higher than δ for Sn. The curve for Pb

TABLE I. Data used to calculate the density effect. Energies are given in Rydberg units.

Material	Li	Be	Graphite	Al	Fe	Cu
$h\nu_1$	5.3	10.9	23.0	115	524	662
$h\nu_2$	0.4	1.0	4.1	6.7	55.3	72.1
$h\nu_3$	1.3	2.4	5.0	5.4
$h\nu_4$	0.9	0.6
f_1	2/3	2/4	2/6	2/13	2/26	2/29
f_2	1/3	2/4	2/6	8/13	8/26	8/29
f_3	2/6	3/13	14/26	18/29
f_4	2/26	1/29
$h\nu_m$	2.22	3.31	5.00	8.18	13.1	14.2
$h\nu_m'$	2.50	4.44	5.67	11.0	17.9	20.5
ν_m'/ν_m	1.13	1.34	1.13	1.34	1.37	1.44
$h\nu_p$	1.01	1.90	2.26	2.43	4.05	4.29
A	0.0661	0.0678	0.0765	0.0737	0.0713	0.0698
B	19.9	18.8	18.3	17.0	16.0	15.7

Material	Ag	Sn	W	Au	Pb	U
$h\nu_1$	1878	2150	5114	5940	6463	8477
$h\nu_2$	260	304	812	975	1053	1419
$h\nu_3$	36.3	46.4	157	193	214	335
$h\nu_4$	4.8	6.4	22.8	24	28.1	51.6
$h\nu_5$	0.6	1.3	3.6	4.1	5.8	11.3
$h\nu_6$	2.8	2.9
f_1	2/47	2/50	2/74	2/79	2/82	2/92
f_2	8/47	8/50	8/74	8/79	8/82	8/92
f_3	18/47	18/50	18/74	18/79	18/82	18/92
f_4	18/47	18/50	32/74	32/79	32/82	32/92
f_5	1/47	4/50	14/74	19/79	18/82	18/92
f_6	4/82	14/92
$h\nu_m$	25.2	26.8	43.8	42.6	45.4	51.9
$h\nu_m'$	31.5	35.2	51.3	54.6	55.6	64.8
ν_m'/ν_m	1.25	1.31	1.17	1.28	1.22	1.25
$h\nu_p$	4.53	3.72	5.90	5.89	4.49	5.69
A	0.0667	0.0644	0.0615	0.0614	0.0606	0.0590
B	14.8	14.6	13.9	13.7	13.7	13.4

Material	H ₂	He	N ₂	Ne	A	Kr	Xe
$h\nu_1$	1.0	1.8	30.3	64	235	1050	2545
$h\nu_2$	3.5	4.0	21.6	129	373
$h\nu_3$	2.3	...	2.9	11.2	61.1
$h\nu_4$	2.9	12.4
$h\nu_5$	1.9
f_1	1	1	2/7	2/10	2/18	2/36	2/54
f_2	2/7	8/10	8/18	8/36	8/54
f_3	3/7	...	8/18	18/36	18/54
f_4	8/36	18/54
f_5	8/54
$h\nu_m$	1.00	1.80	5.38	7.02	11.5	18.3	32.1
$h\nu_m'$	1.15	1.98	6.45	8.85	14.1	25.0	37.4
ν_m'/ν_m	1.15	1.10	1.20	1.26	1.23	1.37	1.17
$h\nu_p$	0.020	0.020	0.053	0.046	0.060	0.085	0.104
A	0.153	0.0765	0.0765	0.0759	0.0698	0.0658	0.0629
B	21.5	20.4	18.0	17.4	16.5	15.3	14.5

Material	Anthracene	Toluene	H ₂ O	AgCl	Emulsion	NaI
$h\nu_1$	23	23	42.3	1878	993	2448
$h\nu_2$	4.1	4.1	4.0	260	120	356
$h\nu_3$	1.3	1.3	2.9	36.3	16	56.6
$h\nu_4$	1.0	1.0	1.0	4.8	2	10.8
$h\nu_5$	0.6	...	1.4
$h\nu_6$	208	...	96
$h\nu_7$	14.8	...	5
$h\nu_8$	4.0	...	0.4
f_1	28/94	14/50	2/10	2/64	2/35	2/64
f_2	28/94	14/50	2/10	8/64	8/35	8/64
f_3	28/94	14/50	4/10	18/64	18/35	18/64
f_4	10/94	8/50	2/10	18/64	7/35	18/64
f_5	1/64	...	7/64
f_6	2/64	...	2/64
f_7	8/64	...	8/64
f_8	7/64	...	1/64
$h\nu_m'$	4.75	4.39	5.00	25.6	21.0	28.8
$h\nu_p$	1.72	1.46	1.58	3.33	2.82	2.65
A	0.0808	0.0831	0.0851	0.0684	0.0708	0.0653
B	18.7	18.8	18.5	15.3	15.7	15.0

lies 0.14 below that for U. NaI and LiI have the same δ within 0.1 as U. This result arises because the smaller Z for iodine which leads to a stronger polarization per electron is compensated by the smaller electronic density of the iodides as compared to uranium.

The values of δ for the cases of gases which were calculated are shown in Fig. 2 with the exception of H₂ at 0.2 atmos. This curve lies close to the curve for

¹² If it is assumed that only the energy loss in the AgBr crystals is detected, the relevant density effect is that for AgBr. [E. Pickup and L. Voyvodic, Phys. Rev. **80**, 89 (1950)]. δ for AgBr is \sim equal to δ for AgCl. The corresponding values of A and B are A = 0.0668 Mev/g cm⁻², B = 15.1.

TABLE II. Values of the coefficients of Eqs. (10) and (10a) for the density correction δ .

Material	$-C$	$10a$	m	x_1	x_0
Li	2.81	3.56	2.99	2	-0.10
Be	2.70	2.60	3.38	2	0.00
Graphite	2.82	3.18	3.15	2	0.04
Al	4.06	0.38	4.25	3	0.39
Fe	3.97	0.88	3.47	3	-0.01
Cu	4.13	0.99	3.40	3	0.00
Ag	4.88	1.62	3.10	3	-0.03
Sn	5.49	2.43	2.85	3	0.17
W	5.33	2.14	2.93	3	0.21
Au	5.45	2.54	2.80	3	0.25
Pb	6.03	3.16	2.71	3	0.38
U	5.86	3.27	2.64	3	0.20
H ₂	9.11	3.4	5.01	3	1.76
He	10.19	9.8	4.11	3	2.00
Ne	11.52	2.17	3.34	4	2.10
A	11.92	3.89	2.80	4	1.96
Kr	12.37	5.37	2.56	4	2.00
Xe	12.77	7.94	2.19	4	1.72
Anthracene	3.03	4.3	2.79	2	0.09
Stilbene	3.03	4.0	2.90	2	0.09
Toluene	3.20	4.6	2.77	2	0.12
Xylene	3.14	4.5	2.77	2	0.12
H ₂ O	3.30	3.77	3.15	2	0.08
AgCl	5.08	1.39	3.30	3	0.18
AgBr	5.14	1.60	3.18	3	0.10
Emulsion	5.02	1.56	3.17	3	0.17
NaI	5.77	2.78	2.77	3	0.09
LiI	5.52	2.77	2.72	3	-0.07
N ₂	10.60	1.12	3.84	4	1.81

N₂. However, δ for H₂ remains zero up to $\log_{10}(p/\mu c) = 2.11$ instead of the cutoff 1.81 for N₂. For large $p/\mu c (> 10^{3.5})$ the H₂ line lies ~ 0.13 below the N₂ line. We note that δ for O₂ lies ~ 0.1 below the N₂ curve, so that the correction for N₂ can also be used for air. Whenever the pressure is not indicated in Fig. 2, the gas is at normal pressure.

In order to give more accurate values of δ , which do not involve the use of Figs. 1 and 2, the calculated values of δ have been fitted by means of an analytic expression as follows:

$$\delta = 4.606x + C + a(x_1 - x)^m, \quad (x_0 < x < x_1) \quad (10)$$

$$\delta = 4.606x + C, \quad (x > x_1) \quad (10a)$$

where $x = \log_{10}(p/\mu c)$ and a, m, C are constants which depend on the substance; x_0 is the value of x which corresponds to the momentum below which $\delta = 0$ [see Eq. (9a)]; x_1 corresponds to the momentum above which the relation between δ and x can be considered to be linear. The linearity of δ at large energies can be seen from Figs. 1 and 2. The linear relationship is given by Eq. (46b) below, from which one obtains

$$C = -2 \ln(\nu_m'/\nu_p) - 1. \quad (10b)$$

The term $a(x_1 - x)^m$ in (10) is introduced in order to correct for the fact that in the intermediate region δ exceeds the asymptotic value, Eq. (10a). By means of a suitable choice of x_1 , the resulting expression was made to fit the calculated values of δ to within 0.2 in all cases, and generally with deviations less than 0.1.

The coefficients a and m were obtained by fitting Eq. (10) to δ at x_0 ($\delta(x_0) = 0$) and at a point near the middle of the range (x, x_1) . Table II gives the values of C, a, m, x_1 needed to evaluate (10), in addition to x_0 . The values given for gases pertain to normal pressure. It can be easily shown that δ at any other pressure P (atmos) can be obtained from δ at $P = 1$ by means of the relation

$$\delta_P(P^{-1/3}p) = \delta_1(p), \quad (10c)$$

where $\delta_{P'}(\lambda)$ denotes δ for a pressure P' and momentum λ . To prove Eq. (10c), we consider Eq. (2) and note that an increase of pressure by a factor P decreases \bar{v}^2 by the same factor. The left side of (2) is $(\mu c/p)^2$. Consider a momentum p for the gas at normal pressure; a certain l corresponds to p . If the pressure is increased and a new value of $l, l' = lP^{-1/3}$, is considered, the left side of (2) corresponds to a momentum $p' = pP^{-1/3}$. In this process the values of $(\bar{v}_i^2 + l^2)/\bar{v}_i^2$ are unchanged and hence the first term of Eq. (1). For $\beta \approx 1$, the second term of δ equals $-l^2(\mu c/p)^2$ which is also constant. Thus $\delta_P(p') = \delta_1(p)$. This relation can be used in all cases of interest, since $\beta \approx 1$.

With the values of δ , the ionization loss dE/dx was

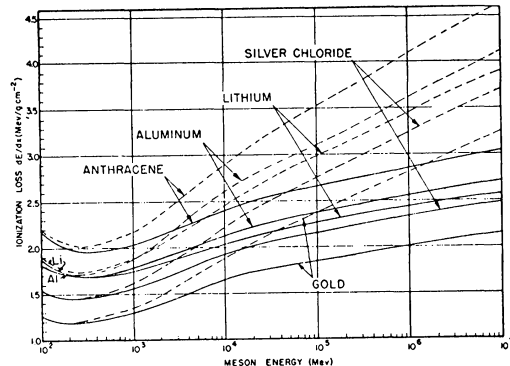


FIG. 3. Ionization loss of μ -mesons in various condensed materials. The broken curve gives the values of $(1/\rho)(dE/dx)$ which would be obtained without the density effect.

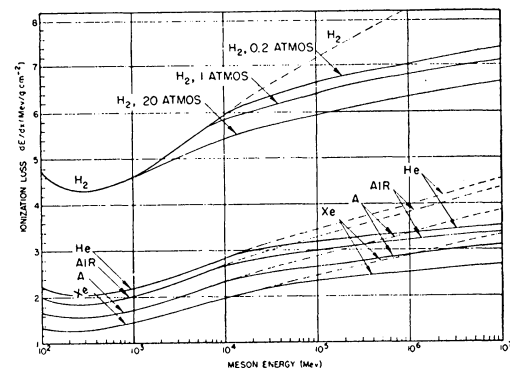


FIG. 4. Ionization loss of μ -mesons in various gases. The broken curves give the values of $(1/\rho)(dE/dx)$ which would be obtained without the density effect.

calculated for several cases. The loss is obtained from the equation¹³

$$\frac{dE}{dx} = \frac{2\pi ne^4}{mv^2} \left[\ln \frac{mv^2 T}{(h\nu'_m)^2(1-\beta^2)} + 1 - \beta^2 - \delta \right], \quad (11)$$

where T is the maximum energy transfer and is given by¹⁴

$$T = \frac{E^2 - \mu^2 c^4}{\mu c^2 (\mu/2m + m/2\mu + E/\mu c^2)}. \quad (12)$$

Here E is the energy of the passing particle, whose mass is μ . For μ -mesons, T approaches asymptotically the value $E - \mu^2 c^2/2m$. For very large $E (E \gg 200\mu c^2)$. For the ionization loss of electrons, one must use

$$T = \frac{1}{2}(E - mc^2) \quad (12a)$$

instead of $E - mc^2$ as given by (12) to take into account the fact that the incident electron and the electron of the atom are indistinguishable.¹⁵ Figures 3 and 4 show the ionization loss of μ -mesons for several solids and gases. For comparison the values of dE/dx which would be obtained without the density effect are also shown (broken curves). Among the solids, anthracene has the largest density effect. Figures 5 and 6 show dE/dx for high energy electrons.

In order to compute the ionization loss, it is useful to write (11) as follows:

$$\frac{1}{\rho} \frac{dE}{dx} = \frac{A}{\beta^2} \left[B + 2 \ln \frac{\dot{p}}{\mu c} + \ln T' + 1 - \beta^2 - \delta \right], \quad (13)$$

where

$$A = 2\pi ne^4/mc^2\rho, \quad (13a)$$

$$B = \ln[mc^2(10^6 \text{ ev})/(h\nu'_m)^2], \quad (13b)$$

T' is the energy transfer in Mev, ρ is the density, so that $(1/\rho)(dE/dx)$ gives the loss per g cm^{-2} . Values of A and B for each substance are given in Table I. At high energies $\beta \approx 1$, and the sum in brackets reduces to four terms. As an example, we calculate dE/dx for μ -mesons of energy 10^5 Mev in uranium. Equation (12) gives $T = 0.91 \times 10^5$ Mev. Using $\mu c^2 = 100$ Mev, one finds $\dot{p}/\mu c = 10^3$ for which Fig. 1 gives a value of $\delta = 7.9$. With $A = 0.0590$ Mev/g cm^{-2} and $B = 13.4$, Eq. (13) gives

$$\begin{aligned} (1/\rho)(dE/dx) &= 0.0590[13.4 + 13.8 + 11.4 - 7.9] \\ &= 1.81 \text{ Mev/g cm}^{-2}. \end{aligned}$$

Equation (13), together with Eq. (12) or (12a) for T , applies to any charged particle. However, for electrons,

¹³ We note that there is some uncertainty concerning the theoretical expression for dE/dx . We choose the same expression as was used by Halpern and Hall (see reference 3) and previously given by W. Heitler, *The Quantum of Radiation* (Oxford University Press, 1936), p. 218, Eq. (1).

¹⁴ H. J. Bhabha, Proc. Roy. Soc. (London) 164, 257 (1937).

¹⁵ W. Heitler, *The Quantum Theory of Radiation* (Oxford University Press, London, 1936), p. 218.

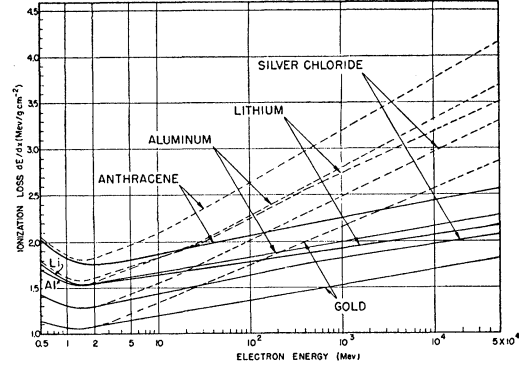


FIG. 5. Ionization loss of electrons in various condensed materials. The broken curves give the values of $(1/\rho)(dE/dx)$ which would be obtained without the density effect.

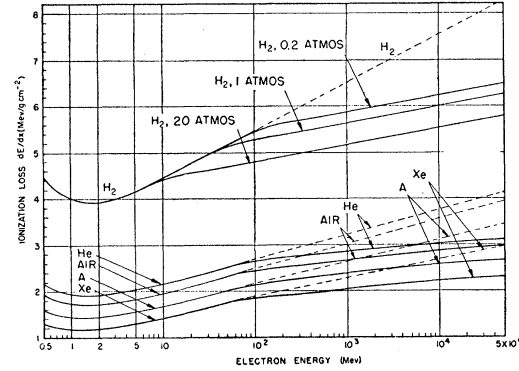


FIG. 6. Ionization loss of electrons in various gases. The broken curves give the values of $(1/\rho)(dE/dx)$ which would be obtained without the density effect.

the result can be somewhat simplified on account of (12a). Thus for electrons of high energy ($\beta \approx 1$), (13) can be written

$$\frac{1}{\rho} \frac{dE}{dx} = A \left[B - 1.4 + 3 \ln \frac{\dot{p}}{mc} - \delta \right]. \quad (14)$$

As an example, dE/dx for 10^3 Mev electrons in U will be calculated. For $\dot{p}/mc = 1960$, Fig. 1 gives $\delta = 9.3$. One finds

$$\begin{aligned} (1/\rho)(dE/dx) &= 0.0590[12.0 + 22.7 - 9.3] \\ &= 1.50 \text{ Mev/g cm}^{-2}. \end{aligned}$$

For low energy electrons ($\beta < 0.95$), the following equation may be used as an alternative to (13),

$$\begin{aligned} \frac{1}{\rho} \frac{dE}{dx} &= \frac{A}{\beta^2} \left[B - 1.4 + 2 \ln \frac{\beta}{(1-\beta^2)^{\frac{1}{2}}} \right. \\ &\quad \left. + \ln \left(\frac{1}{(1-\beta^2)^{\frac{1}{2}}} - 1 \right) + 1 - \beta^2 - \delta \right]. \quad (15) \end{aligned}$$

For high energy particles which lose energy in a thin target there are appreciable fluctuations of the ioniza-

tion loss. The most probable loss is smaller than the average loss given by Eqs. (13) and (14). This effect has been investigated by Landau¹⁶ who found that the most probable loss ϵ_{prob} in a target of thickness t g cm⁻² is given by replacing T in Eq. (11) by $(At/\beta^2)\exp(0.37 + \beta^2)$. Making this substitution in Eq. (13), we obtain

$$\epsilon_{\text{prob}} = \frac{At}{\beta^2} \left[B + 2 \ln \frac{p}{\mu c} + \ln \frac{At}{\beta^2} + 1.37 - \delta \right]. \quad (16)$$

Equation (16) is valid for $T \gg At/\beta^2$ and holds for any charged particle. Thus for a uranium target of thickness 0.5 cm, $t = 9.35$ g cm⁻², the most probable loss of 10^5 Mev mesons is found from Eq. (16) with $At = 0.55$ Mev to be 11.1 Mev, while the average loss ϵ_{av} is $(1.81)(9.35) = 16.9$ Mev. For 10^8 Mev electrons in the same target, $\epsilon_{\text{prob}} = 11.0$ Mev and $\epsilon_{\text{av}} = 14.0$ Mev.

Since we have

$$\delta = C + 2 \ln(p/\mu c) \quad (17)$$

($C = \text{constant}$) for large $p/\mu c$, it is seen from Eq. (13) that dE/dx increases only on account of the term $\ln T'$ at high energies. When T is the full kinetic energy of the passing particle, the extreme relativistic increase of the average loss dE/dx is thus only $\frac{1}{3}$ as fast as it would be without the density effect. This behavior is shown in Figs. 3-6. The most probable loss ϵ_{prob} approaches a finite limit for large energies, as is seen from Eqs. (16) and (17), since the increase of δ just cancels that of $2 \ln(p/\mu c)$. The different behavior of the average and the most probable loss is due to the possibility of a large energy transfer (up to the maximum T) which raises the average energy loss with increasing E but does not affect the most probable loss.¹⁶

The theoretical values of δ for AgCl can be compared with the experiment of Whittemore and Street⁷ on the ionization loss of μ -mesons in a silver chloride crystal. This investigation confirmed the existence of the density effect. On the basis of the most probable loss in the crystal, the authors obtained a curve of the correction δ which when applied to the Bethe-Bloch formula gives best agreement with the experimental results (see Fig. 3 of their paper). The experimental values of δ agree essentially with the curve presented here, although they are larger by ~ 0.8 for large $p/\mu c$ than our values. This discrepancy is quite small and may be due partly to experimental uncertainties as well as to uncertainties in the theoretical expression¹³ for dE/dx used by Whittemore and Street. We conclude that our values of δ for AgCl are in reasonable agreement with experiment.

Bowen and Roser⁷ investigated the response of an anthracene crystal to high energy μ -mesons. They found no rise in ϵ_{prob} with increasing energy in the relativistic region. This result also confirms the existence of the density effect. We note that the curve of

ϵ_{prob} as a function of meson energy, as obtained from Eq. (16) with our values of δ for anthracene has a plateau of ~ 6.0 Mev for meson energies above 500 Mev, in good agreement with the experimental results of Bowen and Roser. Our curve also agrees (within ~ 0.1 Mev) with the ϵ_{prob} curve obtained by these authors, using estimated values for δ .

We have compared our values of δ with those of Halpern and Hall³ in the cases treated by these authors. The present values of δ generally agree with those of Halpern and Hall within 1 unit. The small differences between the two results arise because of the use of different frequencies for the dispersion oscillators. The corresponding values of dE/dx agree with those of Halpern and Hall (obtained with $I = 13.5Z$ ev) within ~ 0.1 Mev/g cm⁻².

III. EQUATIONS FOR THE DENSITY EFFECT

In this section we give the derivation of the equations of the density effect which has been previously obtained.⁵ If the electric field \mathbf{E} of the passing particle and the polarization \mathbf{P} of the medium are Fourier analyzed, a relation

$$\alpha(\omega)\mathbf{E}_\omega = 4\pi\mathbf{P}_\omega \quad (18)$$

is assumed to hold for the Fourier components of frequency ω . $\alpha(\omega)$ is 4π times the polarizability, for which we write

$$\alpha(\omega) = \frac{4\pi n e^2}{m} \sum_i \frac{f_i}{\omega_i^2 - 2i\eta_i\omega - \omega^2}, \quad (19)$$

where the atomic frequencies ω_i , the damping constants $2\eta_i$, and ω are to be expressed in rad/sec. It was shown by Fermi¹ that the ionization loss to atoms with impact parameter greater than b is given by

$$W_b = \frac{2e^2b}{\pi v^2} \text{Rl} \int_0^\infty \left(\frac{1}{1+\alpha} - \beta^2 \right) i\omega k^* K_1(k^*b) K_0(kb) d\omega, \quad (20)$$

where K_0 and K_1 are the modified Bessel functions of the second kind, Rl denotes the real part, and k is the square root with real part ≥ 0 of

$$k^2 = \frac{\omega^2}{v^2} (1 - \beta^2) - \frac{\omega^2 \alpha}{c^2}. \quad (20a)$$

Upon using the approximate expressions for K_0 and K_1 ,

$$K_0(kb) \approx \frac{1}{2} \ln(4/3.17k^2b^2), \quad (21)$$

$$K_1(k^*b) \approx 1/k^*b, \quad (21a)$$

one obtains from Eq. (20)

$$W_b = \frac{4ne^4}{mv^2} \text{Rl} \int_0^\infty \left(1 - \beta^2 - \frac{\alpha}{1+\alpha} \right) \left[\ln \frac{4m^2}{3.17\pi b^2 n e^2 (1 - \beta^2)} - 2 \ln v - \ln \left(1 - \frac{\beta^2 \alpha}{1 - \beta^2} \right) \right] i\nu d\nu, \quad (22)$$

¹⁶ L. Landau, J. Phys. (U.S.S.R.) 8, 201 (1944); K. R. Symon, thesis, Harvard University (1948) (unpublished).

where $\nu \equiv \omega(4\pi n e^2/m)^{-1/2}$. In the following, it is assumed that the damping constants $2\eta_j$ and binding frequencies ν_j are also expressed in units of the plasma frequency, so that the factor $(4\pi n e^2/m)$ of α disappears. In the case where the transition has $\nu_j=0$ (conduction electron), η_j is related to the static conductivity σ as follows:

$$\eta_j = \frac{n f_j e^2}{4\pi m \sigma} \sec^{-1} = \left(\frac{n e^2}{\pi m}\right)^{1/2} \frac{f_j}{4\sigma} \text{ (units } \nu_p). \quad (23)$$

In order to evaluate (22), it is useful to write $\alpha/(1+\alpha)$ as a sum of partial fractions,

$$\frac{\alpha}{1+\alpha} = \sum_i \frac{F_i}{l_i^2 - 2i\xi_i\nu - \nu^2}, \quad (24)$$

where F_i , l_i , $2\xi_i$ are the modified oscillator strength, frequency, and damping constant, respectively, associated with the i th transition. From the expression for α [Eq. (19)] it will be shown that to a good approximation, $F_i = f_i$, $\xi_i = \eta_i$, and

$$l_i = (\nu_i^2 + f_i)^{1/2}. \quad (25)$$

It follows from (25) that $l_i \approx \nu_i$, except for $\nu_i < 1$, i.e., for the transitions from the most loosely bound electrons. In order to prove these results, we consider a simplified case in which the medium can be represented by only two types of dispersion oscillators. The frequency ν_1 (in units ν_p) is assumed $\gg 1$, while $\nu_2 < 1$. From (19) one obtains

$$\frac{\alpha}{1+\alpha} = \frac{f_1(\nu_2^2 - 2i\eta_2\nu - \nu^2) + f_2(\nu_1^2 - 2i\eta_1\nu - \nu^2)}{D}, \quad (26)$$

with

$$D = (\nu_1^2 - 2i\eta_1\nu - \nu^2)(\nu_2^2 + f_2 - 2i\eta_2\nu - \nu^2) + f_1(\nu_2^2 - 2i\eta_2\nu - \nu^2). \quad (26a)$$

Alternatively, Eq. (24) gives

$$\frac{\alpha}{1+\alpha} = \frac{F_1(l_2^2 - 2i\xi_2\nu - \nu^2) + F_2(l_1^2 - 2i\xi_1\nu - \nu^2)}{(l_1^2 - 2i\xi_1\nu - \nu^2)(l_2^2 - 2i\xi_2\nu - \nu^2)}. \quad (27)$$

We equate the denominators of (26) and (27). Equating the coefficients of all powers of ν gives

$$\xi_1 + \xi_2 = \eta_1 + \eta_2, \quad (28)$$

$$l_1^2 + l_2^2 = \nu_1^2 + \nu_2^2 + f_1 + f_2, \quad (29)$$

$$\xi_2 l_1^2 + \xi_1 l_2^2 = \eta_1 \nu_2^2 + \eta_2 \nu_1^2 + \eta_2 f_1 + \eta_1 f_2, \quad (30)$$

$$l_1^2 l_2^2 = \nu_1^2 \nu_2^2 + f_1 \nu_2^2 + f_2 \nu_1^2. \quad (31)$$

These equations are satisfied by $\xi_i = \eta_i$ and by Eq. (25) for l_i . In (31) the assumption that $\nu_i^2 \gg 1$ ($> f_i$) was used. In order to obtain F_i , we equate the numerators of (26) and (27). One finds

$$F_1 + F_2 = f_1 + f_2, \quad (32)$$

$$F_1 \xi_2 + F_2 \xi_1 = f_1 \eta_2 + f_2 \eta_1, \quad (33)$$

$$F_1 l_2^2 + F_2 l_1^2 = f_1 \nu_2^2 + f_2 \nu_1^2. \quad (34)$$

These equations are satisfied by $F_i = f_i$, up to terms of order $f_1 f_2 \ll f_2 \nu_1^2$.

The result of Eq. (25) can be understood by considering the singularity near $\nu = \nu_i$. Near ν_i only the i th term of (19) is of importance, so that

$$\frac{\alpha}{1+\alpha} \approx \frac{f_i(\nu_i^2 - \nu^2)^{-1}}{1 + f_i(\nu_i^2 - \nu^2)^{-1}}, \quad (35)$$

where $\eta_i = 0$ has been assumed for simplicity. The denominator of (35) vanishes for $\nu^2 = \nu_i^2 + f_i$, which agrees with Eq. (24) regarding the singularity at $\nu^2 = l_i^2$. In case there is an oscillator with $\nu_i = 0$, $l_i = f_i^{1/2}$ and (24) becomes 1 near $\nu = 0$, which is seen to be the correct limit from the expression for α . The preceding proof of Eq. (25), which was given for a system of two dispersion oscillators, obviously holds for an arbitrary number, since near each ν_i only the i th term of α matters and the replacement of ν_i by l_i ensures that the singularity of $\alpha/(1+\alpha)$ occurs at the correct ν .

By means of (24) with $F_i = f_i$, $\xi_i = \eta_i$, W_b can be reduced to the following integrals:

$$I_1 = \text{RI} \int_0^\infty i\nu d\nu,$$

$$I_2 = \text{RI} \int_0^\infty i\nu \ln \nu d\nu,$$

$$I_3 = \text{RI} \int_0^\infty i\nu \ln \left[1 - \frac{\beta^2}{1 - \beta^2} \sum_i \frac{f_i}{\nu_i^2 - 2i\eta_i\nu - \nu^2} \right] d\nu,$$

$$I_{4j} = \text{RI} \int_0^\infty \frac{f_j}{l_j^2 - 2i\eta_j\nu - \nu^2} i\nu d\nu,$$

$$I_{5j} = \text{RI} \int_0^\infty \frac{f_j}{l_j^2 - 2i\eta_j\nu - \nu^2} i\nu \ln \nu d\nu,$$

$$I_{6j} = \text{RI} \int_0^\infty \frac{f_j}{l_j^2 - 2i\eta_j\nu - \nu^2} i\nu \times \ln \left[1 - \frac{\beta^2}{1 - \beta^2} \sum_i \frac{f_i}{\nu_i^2 - 2i\eta_i\nu - \nu^2} \right] d\nu. \quad (36)$$

The path of integration is along the positive real axis. These integrals can be evaluated in the manner shown by Fermi¹ by considering the closed contour consisting of the real axis up to a large distance R , a quarter of circle of radius R with center at the origin and the positive imaginary axis from iR to 0. There are no

singularities inside the contour, so that the integral along the real axis is the negative of the integral along the rest of the contour in the counterclockwise direction.

The evaluation of (36) will be illustrated by calculating I_{6j} . For large R , the contribution from the circle is

$$\text{Rl} \int_0^{\pi/2} f_j \ln \left(1 + \frac{\beta^2}{(1-\beta^2)R^2 \exp(2i\theta)} \right) d\theta = O(R^{-2}),$$

which goes to zero as $R \rightarrow \infty$. The integral along the imaginary axis is

$$I_{6j}' = -\text{Rl} \int_{-\infty}^0 \frac{f_j}{l_j^2 + 2\eta_j y + y^2} \times \ln \left[1 - \frac{\beta^2}{1-\beta^2} \sum_i \frac{f_i}{\nu_i^2 + 2\eta_i y + y^2} \right] i y dy. \quad (37)$$

For large y , the bracket > 0 and the integral has no real part. For $y < l$, where l is defined by

$$\frac{1}{\beta^2} - 1 = \sum_i \frac{f_i}{\nu_i^2 + 2\eta_i l + l^2}, \quad (38)$$

the logarithm gives $-i\pi$ so that

$$I_{6j}' = -\pi f_j \int_l^0 \frac{y dy}{l_j^2 + 2\eta_j y + y^2} = \frac{\pi f_j}{2} \ln \left(\frac{l_j^2 + 2\eta_j l + l^2}{l_j^2} \right) - \pi f_j T_{bj}, \quad (37a)$$

where

$$T_{bj} = \frac{\eta_j}{(l_j^2 - \eta_j^2)^{1/2}} \tan^{-1} \frac{l(l_j^2 - \eta_j^2)^{1/2}}{l_j^2 + \eta_j l}, \quad (l_j > \eta_j) \quad (39)$$

$$T_{bj} = \frac{\eta_j}{(\eta_j^2 - l_j^2)^{1/2}} \tanh^{-1} \frac{l(\eta_j^2 - l_j^2)^{1/2}}{l_j^2 + \eta_j l}. \quad (l_j < \eta_j) \quad (39a)$$

The singularities of the integrand are at

$$\nu = -i\eta_i \pm (\nu_i^2 + \eta_i^2)^{1/2}, \quad -i\eta_j \pm (l_j^2 + \eta_j^2)^{1/2}, \quad (40)$$

and lie in the lower half-plane outside the contour. Hence $I_{6j} = -I_{6j}'$.

The condition $l_j > \eta_j$ holds in most actual cases, whereas $l_j < \eta_j$ applies only to conduction electrons ($\nu_j = 0$) in case there is strong damping (poor conductor). The values of I_n are

$$\begin{aligned} I_1 &= I_2 = 0, \\ I_3 &= -\frac{1}{2}\pi l^2 + \frac{1}{2}\pi \beta^2 / (1-\beta^2), \\ I_{4j} &= -\frac{1}{2}\pi f_j, \\ I_{6j} &= -\frac{1}{2}\pi f_j \ln l_j - \frac{1}{2}\pi f_j T_{aj}, \\ I_{6j} &= -\frac{1}{2}\pi f_j \ln [(l_j^2 + l^2 + 2\eta_j l) / l_j^2] + \pi f_j T_{bj}, \end{aligned} \quad (41)$$

where

$$T_{aj} = \frac{\eta_j}{(l_j^2 - \eta_j^2)^{1/2}} \tan^{-1} \frac{(l_j^2 - \eta_j^2)^{1/2}}{\eta_j}, \quad (l_j > \eta_j) \quad (42)$$

$$T_{aj} = \frac{\eta_j}{(\eta_j^2 - l_j^2)^{1/2}} \tanh^{-1} \frac{(\eta_j^2 - l_j^2)^{1/2}}{\eta_j}. \quad (l_j < \eta_j) \quad (42a)$$

From Eq. (22) one finds

$$W_b = \frac{4\pi e^4}{mv^2} \left[I_3(\beta^2 - 1) - \sum_j I_{4j} \ln \frac{4mv^2}{3.17\pi b^2 n e^2 (1-\beta^2)} + \sum_j (2I_{6j} + I_{6j}) \right]. \quad (43)$$

Upon inserting the values (41) into (43) one obtains

$$W_b = \frac{2\pi n e^4}{mv^2} \left[\ln \frac{4mv^2}{3.17\pi b^2 n e^2 (1-\beta^2)} - \sum_j f_j \ln (l_j^2 + l^2 + 2\eta_j l) - \sum_j 2f_j (T_{aj} - T_{bj}) + l^2(1-\beta^2) - \beta^2 \right]. \quad (44)$$

The density effect is obtained by comparing W_b with the classical ionization loss W_{b0} to a system of isolated atoms which is given by¹⁰

$$W_{b0} = \frac{2\pi n e^4}{mv^2} \left[\ln \frac{4mv^2}{3.17\pi b^2 n e^2 (1-\beta^2)} - \beta^2 - \sum_j f_j \ln \nu_j^2 \right]. \quad (45)$$

The reduction of the ionization loss is

$$W_{b0} - W_b = \frac{2\pi n e^4}{mv^2} \left[\sum_j f_j \ln \left(\frac{l_j^2 + l^2 + 2\eta_j l}{\nu_j^2} \right) + 2 \sum_j f_j (T_{aj} - T_{bj}) - l^2(1-\beta^2) \right]. \quad (46)$$

Since damping of the dispersion oscillators is not taken into account in W_{b0} , Eq. (46) gives the combined effect of the polarization and damping.³ For $\beta < \beta_0$ [see Eq. (9a)], $l = 0$ and one obtains only a small effect

$$W_{b0} - W_b = \frac{2\pi n e^4}{mv^2} \left(\sum_j f_j \ln \left(\frac{l_j^2}{\nu_j^2} \right) \right). \quad (46a)$$

For the case of a single dispersion oscillator, Eq. (46a) gives $(2\pi n e^4 / mv^2) \ln \epsilon$, where ϵ is the static dielectric constant. This agrees with Fermi's result.¹ For very high energies, $l = (1-\beta^2)^{-1/2}$ and we obtain

$$W_{b0} - W_b = \frac{2\pi n e^4}{mv^2} \left[-\ln(1-\beta^2) - \sum_j f_j \ln \nu_j^2 - 1 \right], \quad (46b)$$

in agreement with the results of Fermi¹ and others.^{3,4}

Equation (46) for the density effect is valid for an arbitrary number of dispersion oscillators, each having its own binding and damping characteristics. The l_j can be taken as the excitation frequencies ν_j , except for the conduction electrons for which $l_j = f_j^{\frac{1}{2}}$ should be used. The damping terms T_{aj} , T_{bj} are obtained from Eqs. (39) and (42), and l is obtained by solving (38).

In the case in which damping can be neglected for all but one transition ($j = j_0$) and if $\eta_{j_0} \gg l_{j_0}$, we have

$$T_{aj_0} - T_{bj_0} \approx \frac{1}{2} \ln(1 + 2\eta_{j_0}/l),$$

$$W_{b_0} - W_b = \frac{2\pi n e^4}{m v^2} \left[\sum_{j \neq j_0} f_j \ln \left(\frac{l_j^2 + l^2}{\nu_j^2} \right) + f_{j_0} \ln \left(\frac{l + 2\eta_{j_0}}{\nu_{j_0}} \right)^2 - l^2(1 - \beta^2) \right]. \quad (47)$$

If $\nu_j > 1$ for $j \neq j_0$, l_j can be replaced by ν_j and the result agrees with that of Halpern and Hall.¹⁷ We note that the η_{j_0} term makes a sizable contribution to $W_{b_0} - W_b$ if f_{j_0} is appreciable. This contribution does not become zero for low energies when $l = 0$. The η_{j_0} term corresponds to the fact that a strong damping is equivalent to a binding in reducing the ionization loss.

When the mean excitation frequency ν_m' is determined experimentally as in the work of Bakker and Segrè,¹¹ ν_m' includes the effect of damping so that the δ , which must be applied to the Bethe-Bloch formula with the experimental ν_m' , should become zero at low energies. The procedure used in the calculations of Sec. II in which it was assumed that $\eta_i = 0$ gives zero correction at low energies (when $l = 0$). In all cases (see Table I), the excitation frequencies ν_j exceed $f_j^{\frac{1}{2}}$ so that $l_j \approx \nu_j$. Thus Eq. (46) reduces to Eq. (1) which was used in the numerical work.

Halpern and Hall³ have considered the effect of the Lorentz term in the dielectric constant. Thus the

¹⁷ See Eq. (17) of reference 3.

polarizability upon inclusion of this term becomes

$$\alpha(\nu) = \frac{\sum_{j \neq j_0} \frac{f_j}{\nu_j^2 - 2i\eta_j\nu - \nu^2}}{1 - \frac{1}{3} \sum_{j \neq j_0} \frac{f_j}{\nu_j^2 - 2i\eta_j\nu - \nu^2}} + \frac{f_{j_0}}{-2i\eta_{j_0}\nu - \nu^2}, \quad (48)$$

where j_0 is the transition, if present, for which $\nu_j = 0$. If we let $f_j' \equiv -f_j/3$, we may write

$$\alpha(\nu) = -3 \frac{\zeta}{1 + \zeta} + \frac{f_{j_0}}{-2i\eta_{j_0}\nu - \nu^2}, \quad (49)$$

where

$$\zeta = \sum_{j \neq j_0} \frac{f_j'}{\nu_j^2 - 2i\eta_j\nu - \nu^2}. \quad (49a)$$

The first term of (49) is of the same form as $\alpha/(1 + \alpha)$. Corresponding to the results obtained above [see Eqs. (24) and (25)], we find

$$\frac{\zeta}{1 + \zeta} \approx \sum_{j \neq j_0} \frac{f_j'}{\tilde{\nu}_j^2 - 2i\eta_j\nu - \nu^2}, \quad (50)$$

where

$$\tilde{\nu}_j = (\nu_j^2 + f_j')^{\frac{1}{2}} = (\nu_j^2 - f_j/3)^{\frac{1}{2}}. \quad (j \neq j_0) \quad (51)$$

Upon inserting (50) into (49) it is seen that the effect of the Lorentz term is merely to replace ν_j by $\tilde{\nu}_j$, except when $\nu_j = 0$ in which case ν_j must still be used. The resulting equation for l_j is

$$l_j = (\tilde{\nu}_j^2 + f_j)^{\frac{1}{2}} = (\nu_j^2 + \frac{2}{3}f_j)^{\frac{1}{2}}. \quad (j \neq j_0) \quad (52)$$

Equation (46) with l_j as obtained from (52) gives the density effect when the Lorentz term is taken into account. However, since in all cases of Sec. II, the difference between l_j and ν_j could be neglected, we may conclude that the Lorentz correction is also unimportant for these cases.

I would like to thank Dr. Ernest D. Courant for several very helpful discussions and comments. I am also indebted to Dr. W. L. Whittemore for information concerning his experiment.